

Intracavity laser absorption spectroscopy using mid-IR quantum cascade laser

G. Medhi^a, A. V. Muravjov^b, H. Saxena^b, C. J. Fredricksen^a, T. Brusentsova^a, R. E. Peale^a, O. Edwards^b

^aDepartment of Physics, University of Central Florida, Orlando, Florida, 32816 USA

^bZyberwear Inc. 2650 Florence Street, Orlando, Florida, 32818 USA

ABSTRACT

Intracavity Laser Absorption Spectroscopy (ICLAS) at IR wavelengths offers an opportunity for spectral sensing with sufficient sensitivity to detect vapors of low vapor pressure compounds such as explosives. Reported here are key enabling technologies for this approach, including multi-mode external-cavity quantum cascade lasers and a scanning Fabry-Perot spectrometer to analyze the laser mode spectrum in the presence of a molecular intracavity absorber. Reported also is the design of a compact integrated data acquisition and control system. Applications include military and commercial sensing for threat compounds, chemical gases, biological aerosols, drugs, and banned or invasive plants or animals, bio-medical breath analysis, and terrestrial or planetary atmosphere science.

Keywords: Intracavity, quantum cascade laser, Fabry-Perot, infrared, spectroscopy.

1. INTRODUCTION

Absorption spectroscopy is one of the most important techniques for the detection and characterization of vapors and gases. This technique involves the measurement of the spectral extinction of the transmitted light through the sample, which is governed by the well-known Lambert-Beer law [1]. For a low vapor pressure sample, such as explosives, the optical path needed to get a sufficient sensitivity by this technique, is more than a kilometer, which is usually impractical. An opportunity is Intracavity Laser Absorption Spectroscopy (ICLAS) at Mid- to Long-wave IR (3-20 μm wavelengths) using quantum cascade lasers (QCL). ICLAS provides effective optical path lengths exceeding a kilometer in a device with centimeter dimensions. Our approach is based on multimode external-cavity QCLs with a rapid-scanning Fabry-Perot interferometer to analyze their spectrum in real time. The emission spectrum of a multimode laser is very sensitive to selective extinction in its cavity, enabling unprecedented sensitivity to ultra trace vapors. Applications include military and commercial screening for threat compounds and contraband including explosives, chemical gases, biological aerosols, drugs, and banned or invasive plants or animals. Also, bio-medical breath analysis and analysis of planetary atmospheres by space probes are envisioned.

2. EXPERIMENT AND RESULTS

2.1 External cavity QCL

A key enabler for the proposed technology is an external cavity quantum cascade laser (QCL). An 8.1 μm QCL from Maxion with one end facet high-reflection coated and the other anti-reflection coated was used with a 90° off axis gold coated parabolic mirror and a flat mirror with an outcoupling aperture. Fig 1 (left) presents the schematic of the system, showing that the external cavity is formed by the high reflecting end facet of the QCL chip and the external flat mirror.

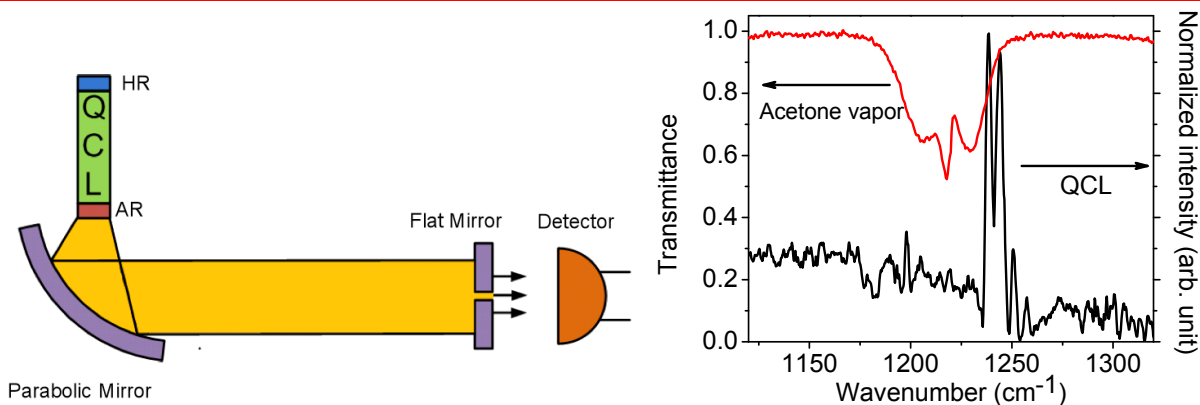


Fig 1 (left) Schematic of external cavity QCL. (right) Transmittance spectrum of acetone vapor, at few Torr pressure in a 10 cm gas cell, compared with external-cavity QCL spectrum.

2.1.1 External cavity sensing demonstration

The QCL wavelength was chosen to coincide with the 8.1 μm absorption band of acetone. This solvent has high vapor pressure, which is favorable for a first vapor-detection demonstration and subsequent system optimization. Fig. 1 (right) compares the transmission spectrum of acetone, measured at a pressure of a few Torr in a 10 cm gas cell [2], to a low-resolution emission spectrum of the external-cavity QCL. Both spectra were collected using a Bomem DA8 Fourier spectrometer. Though the laser operates on the shoulder of the band, where the absorption is considerably weaker, it is sufficient to demonstrate detection of acetone vapor, as shown below.

Fig. 2 presents a photograph of the external-cavity QCL. The external cavity mirror is located ~ 30 cm from the QCL. This gold coated mirror has a hole at its center for output coupling to the 77 K HgCdTe detector. When the alignment is right, the laser starts to oscillate, the detector saturates, and the beam is found to be collimated with a diameter of about 1 cm.

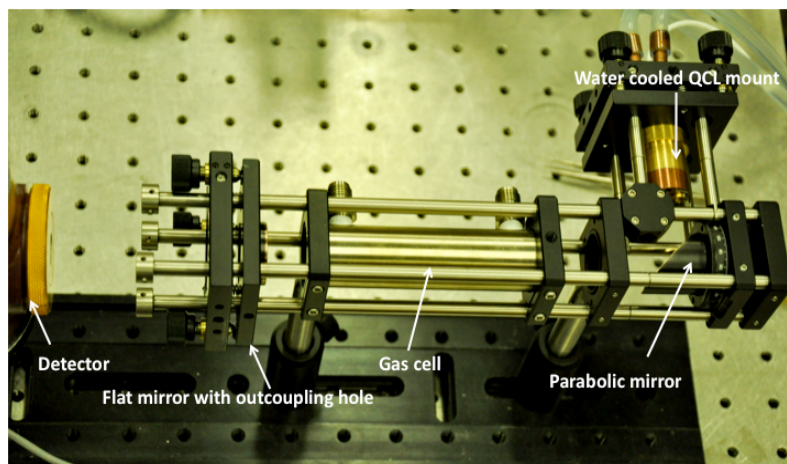


Fig. 2: Photograph of external cavity QCL

Fig. 3 presents the effects of various absorbers on the total laser intensity. The laser was operated near threshold and an excitation pulse of 0.8 ms. The detector was initially saturated, but the emission intensity drops as the laser chip heats due to the drive current. When a polyethylene (PE) sheet was placed in front of the detector but external to the cavity, the signal dropped by $\sim 10\%$ due to single pass absorption by the PE. However, when the PE sheet was placed inside the

cavity, the lasing was almost completely extinguished. The signal with acetone vapor inside the cavity was also strongly attenuated, though by less. These results show that an intracavity absorber with 10% single pass loss causes nearly complete laser extinction. Similarly, unsaturated acetone vapor weakly confined in a ~ 10 cm cell also gives a nearly complete laser extinction. From Figs. 1 and 3, we estimate the unsaturated vapor pressure of acetone to have been ~ 1 Torr. The projected sensitivity limit for acetone based on the attenuation of the total power using this set-up was ~ 0.1 Torr. Based on observed laser intensity variations using our pulsed QCL driver, we estimate that the sensitivity can be increased to $\sim 10^{-4}$ Torr using a more stable laser driver designed for longer pulse operation. Further increases in sensitivity will follow when the sensing is based on the changes to the laser emission spectrum, which is the intended mode of operation. This already makes the device capable of detecting the saturated vapor pressure of TNT at room temperature. Additional sensitivity increases will be obtained by operating the laser continuous wave rather than pulsed, which will substantially increase the effective IR path length.

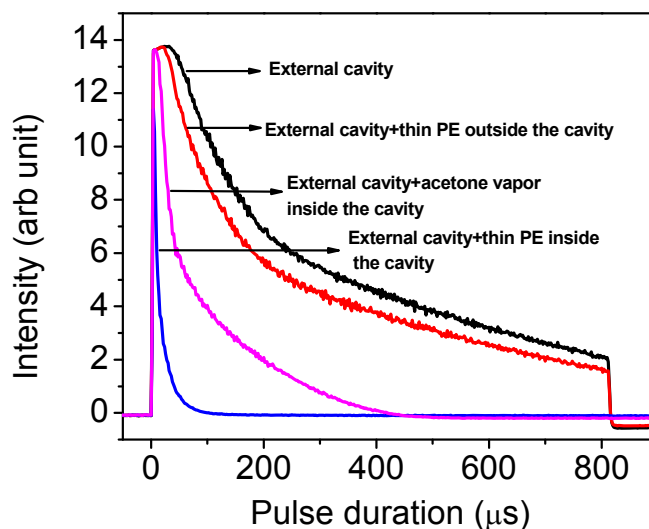


Fig. 3. Oscilloscope traces showing effects on recorded laser intensity of extra- and intra-cavity absorption.

2.1.2 High resolution spectroscopy of external cavity configuration

High resolution spectroscopy was performed using the Fourier spectrometer to see the fine mode spectrum expected of the external cavity configuration. The laser was operated using an ultra stable laser driver (ILX Lightwave, LDX3232). Fig. 4 presents the obtained spectrum. The lower frequency structure of the spectrum presented in Fig. 4 (left) shows clear evidence of periodic mode structure with mode separation of 0.55 cm^{-1} . This structure arises due to feedback reflections from the output facet of the QCL chip. However, due to the AR coating on this facet, this structure practically vanishes on the high frequency side of the emission. The expected mode separation for the cold 33 cm long external cavity for this experiment is 0.015 cm^{-1} . Despite the close match of the best spectrometer resolution of 0.017 cm^{-1} , these modes were unresolved in Fig. 4 (left) due to existence of multiple higher order transverse modes. However, installation of a 10 mm diaphragm within the cavity causes the fine mode structure to appear by extinguishing the higher order transverse modes. Fig. 4 (right) presents a detail of the spectrum on the low-wavenumber shoulder of the emission spectrum. One sees a regular periodic pattern of modes characterized by strong single peaks separated by slightly weaker double peaks. The observed fine mode structure includes typical mode spacing of 0.03 cm^{-1} , corresponding to even modes of the cold resonator.

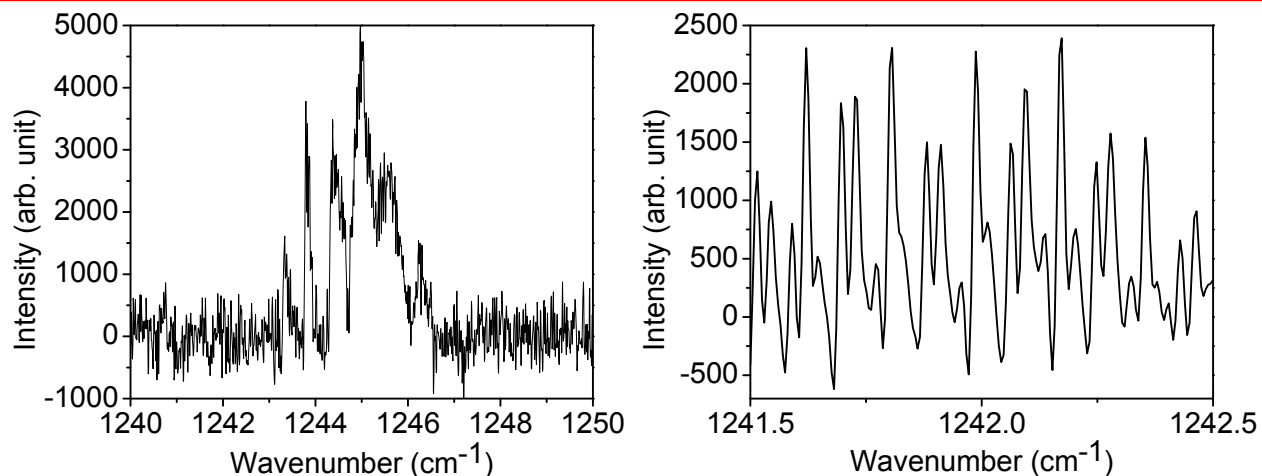


Fig. 4 (left). Emission spectrum of 8.1 μm wavelength QCL with external cavity. Spectral resolution = 0.017 cm^{-1} . Laser current = 875 mA, rep rate = 10 Hz, and pulse duration = 2 ms. (right). Fragment of high-resolution 8.1 μm QCL external cavity mode structure under the same operating conditions but with the addition of a 10 mm intracavity aperture.

2.1.3 Effect of intracavity elements on the system performance

Fig 5 (left) presents the Q-spoiling effect on the high-resolution spectrum when a high purity 1 mm thick uncoated Si etalon is placed inside the cavity. The laser still operates despite the $\sim 20\%$ losses due to reflection from the Si surfaces. Laser operation showed little sensitivity to the exact orientation of the Si spacer with respect to the beam, indicating that the reflected radiation was not coupled back into the laser active medium. Strong mode selection caused by Fabry-Perot interference inside the Si etalon indicates fast development of mode competition during the time of the $\sim 2\ \mu\text{s}$ laser pulse. Even though the period of FP transmission modulation of the silicon spacer is rather wide, with an even resonance spacing of $\sim 1.3\text{ cm}^{-1}$, small differences in transmission of close external cavity QCL modes separated by 0.03 cm^{-1} suffices to suppress all neighboring modes, leaving only 1-2 dominating modes in the center of each transmission maximum, as seen in Fig 5 (right).

Consequently, even the low finesse of a silicon flat (~ 8) suffices to select the laser wavelength with an active cavity resolving power Q of order $\sim 1200\text{ cm}^{-1}/0.03\text{ cm}^{-1} = 40000$. The Q of the 1 mm thick passive silicon flat itself is only 850. This is promising for the potential of achieving high Q tunable wavelength selection and tuning with an intracavity scanning FP.

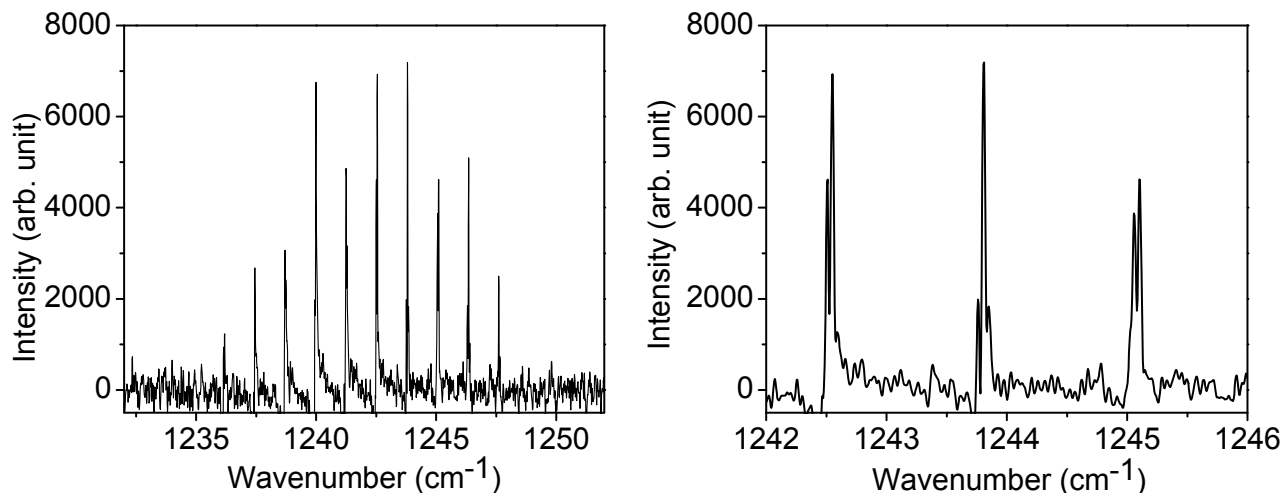


Fig. 5 (left). High resolution emission spectra for the laser with external cavity with intracavity Si spacer. (right) Fragment of high resolution emission spectrum with intracavity Si etalon. The spacing between frequency separation bands is 1.3 cm^{-1} . Individual fine structure mode separation is $\sim 0.03 \text{ cm}^{-1}$ and is due to the longitudinal modes of the external cavity.

Note that the free spectral range of the silicon etalon is 10 times too small to be useful as a selector, because 10 wavelengths within the $\sim 13 \text{ cm}^{-1}$ gain band width of this particular QCL have been selected simultaneously. If the thickness of the silicon flat were reduced from 1 mm to $100 \mu\text{m}$, only a single wavelength would be selected.

Demonstration of the system operation with an intracavity Si etalon has the following significance: 1) It must be possible to use normal incidence (as opposed to Brewster angled) windows for an intracavity gas cell, if the window is thick enough to allow FP resonances to be ignored, or if it has AR coatings, or if it is wedged and has AR coatings. 2) It should be feasible to install a piezo-controlled FP interferometer inside the cavity to achieve a continuously tunable single mode laser. Such, may be competitive with usual grating tuned external cavity QCL designs.

2.1.4 Sensitivity of the system to absorbing elements and vapors inside the cavity

Monitoring changes in the fine mode spectrum of the laser system caused by the presence of a frequency dependent intracavity absorber may remarkably increases the sensitivity of the system in comparison to monitoring the laser intensity only. Fig. 6 demonstrates how the laser emission spectrum operated in continuous wave (CW) mode reacts on the presence of a vapor inside the cavity. In our particular case the laser broadband gain overlaps with acetone absorption shoulder in the 1230 to 1260 cm^{-1} wavenumber range (Fig.1 (right)), which has monotonous frequency dependence with more pronounced absorption in the 1235 - 1245 cm^{-1} spectral range. The laser was operated in the CW mode at the active chip temperature of $\sim 14^\circ\text{C}$. Though the laser threshold current is 920 mA at this operation temperature, the current was set to 940 mA , to avoid instabilities arising from the temperature variation in the chip near the threshold. The concentration of acetone vapor has been chosen below the level when remarkable drop of the laser intensity occurs. Here, a cotton ball soaked in acetone and then dried for half an hour was placed above the open cavity, such that vapors flow down into the cavity. In response to the vapor, the laser emission shifted strongly (by 6 cm^{-1}) away from the absorption toward higher frequencies, even to a region where no laser emission was previously observed. This strongly non-linear behavior demonstrates the extreme sensitivity of the system to frequency dependent intracavity absorbers. The sensitivity of the system can be enhanced further by controlling the laser cooling temperature.

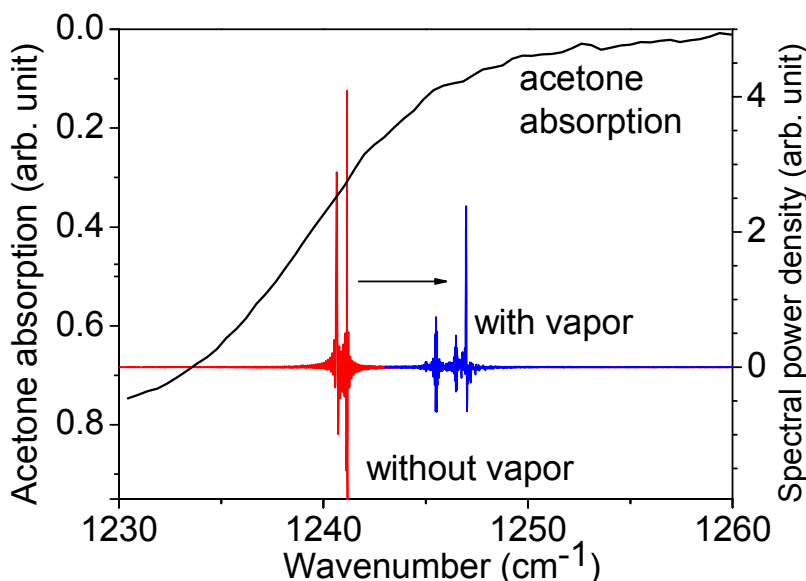


Fig. 6. Emission spectrum of the external cavity QCL with and without presence of acetone vapor. The QCL was operated in CW at 940 mA . The spectral resolution for the laser spectrum was 0.017 cm^{-1} . When the open laser cavity is exposed to room air that contains some acetone vapor, the spectrum blueshifts, as indicated by the arrow.

2.2 Fabry-Perot Spectrometer

The second enabler is a real-time compact high resolution spectrometer. We have developed a scanning Fabry-Perot (FP) spectrometer with a pair of mirrors formed from wedged (30-arcmin) ZnSe flats of 2 mm thickness, with high reflection coatings (97.5%) on the facing surfaces, and AR coatings on the other surfaces. One of the mirrors was fixed, while the other was placed in a mount with high-precision 3-axis alignment and piezo drivers. The piezo was controlled by a three-channel piezo driver. A 9.38 μm wavelength QCL (Alpes) was installed in the focus of the 90-degree off-axis parabolic mirror, which provided a collimated beam for the FP spectrometer. The signal transmitted by the FP was detected by a liquid nitrogen cooled MCT detector and was synchronously amplified. A linear ramp voltage of 0-10V at a rep rate of ~ 10 Hz controlled the piezo driver for the FP.

The signal transmitted by the FP vs mirror displacement is presented in Fig. 7 when the laser was operated under broad band conditions and compared with the full FTIR spectrum. The FP spectrum corresponds to the 25th order of resonance. The spectrum showed good agreement with the FTIR spectrum. The shoulders at the beginning and end of the FP spectrum arise from the overlap of different resonance orders, but the individual modes are still resolved. We estimate that here the achieved resolution is better than 0.5 cm^{-1} , which suffices for the expected pressure broadened vapor line widths of at least 0.2 cm^{-1} .

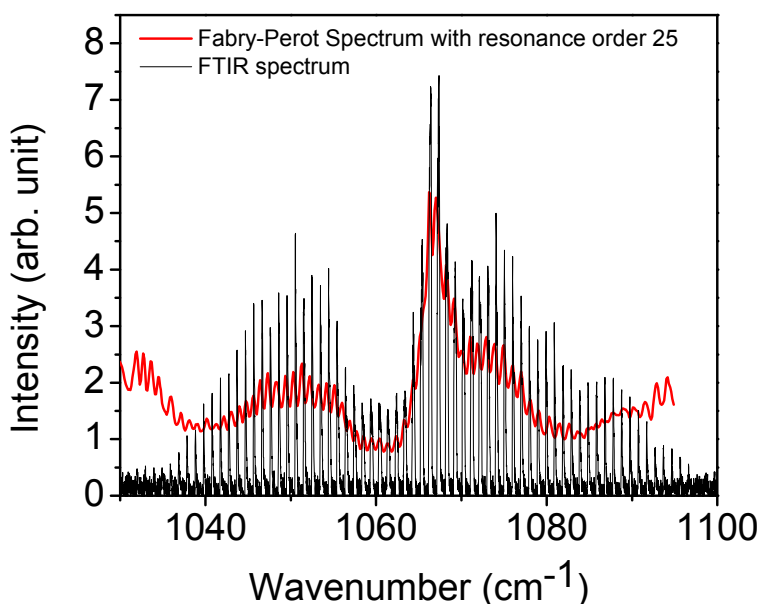


Fig. 7. Comparison of broad-band QCL spectrum measured on Fabry-Perot and Fourier spectrometer.

2.3 Electronics

As part of the first commercial prototype, compact integrated control and data acquisition electronics have been implemented. Fig. 8 presents a photograph of the compact real-time (cRIO) architecture from National Instrument adopted as a development platform.

A single program running on the FPGA module controls the motion of the 3 axes of the piezo stages from a single amplifier (VF-90-30150). The control voltage is in the form of a modified sine wave. The voltage is changed (increased/decreased) linearly through most of the range from 0 to 3.75V. Around the turning points (near 0 and 3.75V), the voltage is changed more slowly (in the form of a sine wave). The waveform is a triangular wave with the sharp corners replaced by sine wave sections. The frequency of the waveform is adjustable in order to control the scanning speed of the piezo driven mirror. The FPGA program also provides square pulses to the QCL driver. This function replaces the DG535 pulse generator previously used, and has the added advantage of higher voltage output (the DG535 was limited to ~ 4 V); the laser driver is more stable being driven with ~ 5 V pulses. The duration and repetition rate of

these pulses are adjustable. The FPGA program also controls data acquisition through two inputs of the NI 9223 analog input module plugged into the cRIO chassis. Each input of this module is capable of simultaneously acquiring data at a maximum rate of 1MS/s. One channel monitors the output of the voltage waveform controlling the position of the piezo driven mirror, and a second channel samples the detector. The FPGA program controls all of the above functions with highly precise timing and essentially no latency. For the purposes of testing various configurations of the laboratory model, another program runs on a personal computer to allow interactive adjustments to be made to the adjustable parameters outlined above (piezo control voltage, laser driver control pulses, sampling rates for the analog inputs). Likewise, the p.c. interface program allows the data from the analog inputs to be plotted. The position (piezo voltage) is plotted in the x-axis and the signal from the detector is plotted in the y-axis. So, the signal from the detector is plotted as a function of the position of the mirror and the spectrum is displayed on the computer monitor.

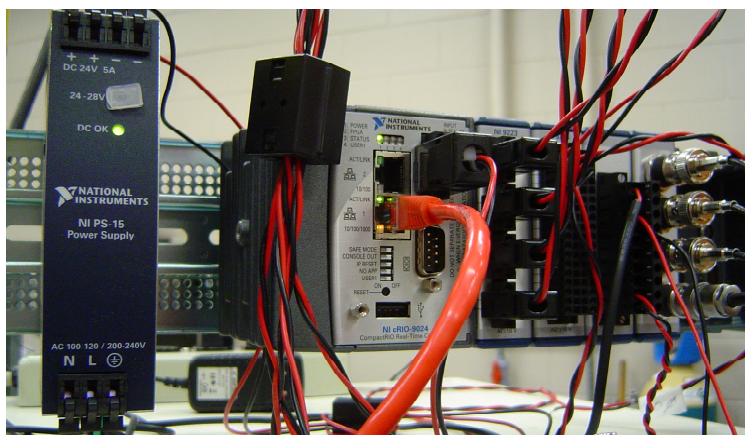


Fig. 8. Photograph of a compact cRIO electronics development platform

The only electronics left external to the cRIO are the laser driver and the cooling control (still under development). The final product will have fixed parameters, such as piezo scanning speed and laser pulse repetition rate, with the possible exception of pre-programmed selectable range adjustments that can be made by toggle switches, etc. on the unit. After integration of the laser driver and cooling controller, the last step will be to determine the logical processes required for recognizing and reacting to various chemical/biological spectra. For the purposes of testing we rely on our human filter modules to recognize features of the spectra displayed on the computer monitor; the commercial product will have built-in logic for recognition of chem/bio threats and warning lights/alarms for the operator.

3. SUMMARY

For LWIR ICLAS system, the key enabling technology is the multimode quantum cascade laser. Equally important is the Fabry-Perot spectrometer to measure the multi-mode emission spectrum at high resolution in real time. An external-cavity QCL and Fabry-Perot operations were clearly demonstrated here. The compact electronics system was also integrated with the optical and spectroscopic techniques.

ACKNOWLEDGEMENT

This project is supported by an Army Phase II SBIR and by an award from the Florida Space Grant Consortium.

REFERENCES

- [1] V. M. Baev, T. Latz, and P. E. Toschek, "Laser intracavity absorption spectroscopy," Appl. Phys. B 69, 171-202 (1999).
- [2] R. E. Peale, A. V. Muravjov, C. J. Fredricksen, G. D. Boreman, H. Saxena, G. Braunstein, V. L. Vaks, A. V. Maslovsky, S. D. Nikifirov "Spectral signatures of acetone from ultraviolet to millimeter wavelengths," Proc. 2006 Intl. Symp. Spectral Sensing Research, May 29 to Jun 2, 2006, Bar Harbor, Maine.